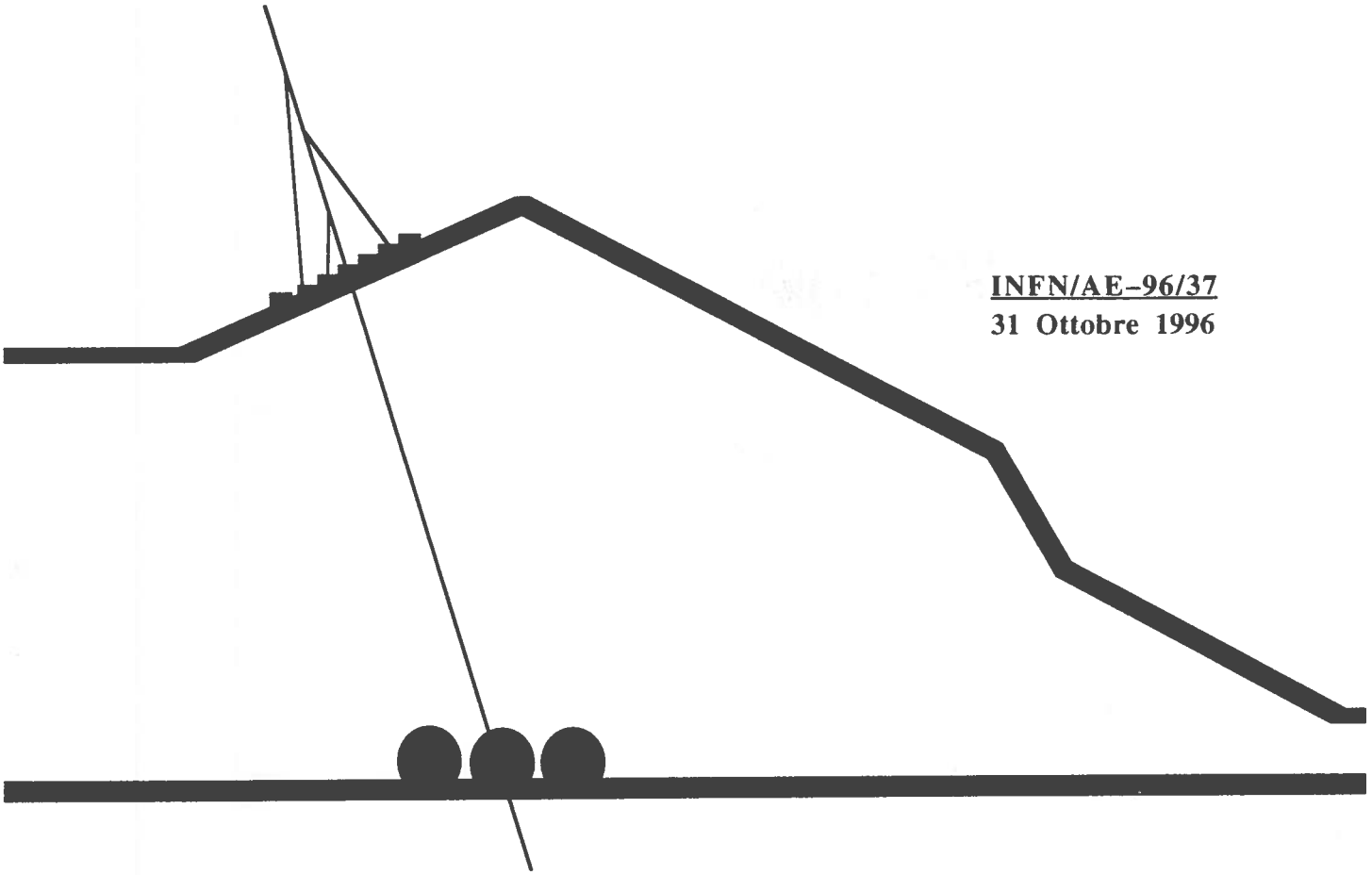

INFN/AE-96/37
31 Ottobre 1996

Extensive Air Showers and Hadronic Interactions

G.Battistoni

Presented at the
1996 Vulcano Workshop on Frontier Objects in Astrophysics and Particle Physics
May 27 – June 1, 1996

INFN - Laboratori Nazionali del Gran Sasso

Published by **SIS–Pubblicazioni**
dei Laboratori Nazionali di Frascati

INFN – Istituto Nazionale di Fisica Nucelare
Laboratori Nazionali del Gran Sasso

INFN/AE–96/37
31 Ottobre 1996

Extensive Air Showers And Hadronic Interactions

G. Battistoni
INFN, Sezione di Milano, via Celoria 16, 20133 Milano, Italy.

Abstract

The main aspects of hadronic interaction affecting the development of Extensive Air Showers are summarized, together with the general problematics of model building. Some results from experience in the study of Cosmic Ray cascades obtained using the DPMJET–II model at E>10^{14} eV are presented. Emphasis is given to the question of nucleus-nucleus interaction, and to the possible overcome of superposition model. The relevance of a few uncertainties, such those due to cross sections and structure functions, are also discussed.

1 Introduction

Indirect measurements addressing the fundamental question of Ultra and Extreme high energy cosmic rays are performed recording the features of different components of the Extensive Air Showers in atmosphere. Interpretation of these data in view of parameters of astrophysical interest, like elemental composition as a function of energy, depends on the hadronic interaction models available for the analysis. On the other hand, this can be interpreted not just as a limitation, but also as an interesting opportunity from the point of view of particle physics. We are able to observe the cosmic rays of the highest energies only through their interaction with the Earth's atmosphere: the reliability of our interpretation of the features of such secondary particles, and of their relation to the characteristics of the primary particle, is necessarily related to quality of our understanding of hadron-hadron, hadron-nucleus and nucleus- nucleus interactions. This aspect is particularly stimulating for high energy physicists, since there is not yet an exact way to calculate the properties of the bulk of hadronic interactions. Also, from the experimental point of view, the productions of secondary cosmic rays at very high energies occurs in kinematic regions, or energy ranges, that have not been explored in accelerator experiments, and that will hardly be accessed even at the hadron colliders of the next generation. Therefore, EAS of energy $> 10^{15}$ still represent an almost unique chance to test our theoretical achievements in very high energy nuclear physics, not to speak of the region above 10^{17} eV, which remains completely out of reach of present accelerator technology. In this review, the relevant aspects of hadronic interactions affecting the EAS development are summarized (Section 2). In Section 3 the general requirements of computable models are discussed, with reference to the experience with the DPMJET–II code. The attention is concentrated on the nucleus–nucleus interactions. In Section 4, a summary of open problems is presented.

2 EAS development and the features of hadronic interactions

In order to delimit the argument of discussion, let us first describe qualitatively what happens when a primary nucleus interacts in the high atmosphere. After an average depth λ_A, the nucleus interacts, but typically only few nucleons participate in the interactions. The "spectator" nucleons break-up in some fragments that will in turn interact, producing additional spectator fragments. This process is iterated until all nucleons will eventually interact. This has to be described by detailed nuclear models; however, for most purposes, in particular at high energy, it is customary to rely on the simple superposition model: a nucleus of mass number A and total energy E_0, behaves as a beam of A independent nucleons each one having energy E_0/A and interaction length λ_N. Each nucleon will interact with the target nuclei of the atmosphere producing many hadrons in the final state. Each hadron particle will go on interacting again with the atmosphere or decaying into other particles. At very high energy the typical interaction length of a nucleon in air is about 80 g/cm^2, while a heavy nucleus can interact after only few g/cm^2. We have then the evolution of a hadronic shower of particles, which develops completely since the atmosphere is ≈ 13 interaction lengths deep, for protons. At each initial step in the shower process the number of particles will grow while the average energy will

decrease. Thus, the number of particles (or, with less ambiguities in the definition, the quantity of energy transferred to secondaries and eventually released in the atmosphere) will reach a maximum at some depth which is a function of energy, of the nature of the primary particle and of the details of the interactions of the primaries and secondaries in the cascade. Most of the produced particles in each hadronic interaction are π and K mesons which can decay into muons (and neutrinos) before interacting, thus producing the most penetrating component of the atmospheric showers. The lateral extension of this component depends on the average transverse momentum of the hadronic parents. Neutral pions decay immediately into photons which initiate electro-magnetic showers.

The basic ingredients for the understanding of showers are the total cross section nucleon-Air (and in general hadron-Air, related to the interaction length) and the differential cross section for multiparticle production. When we speak of total cross section, we should better specify that we are interested in the inelastic part of it, since elastic scattering does not contribute to the processes relevant for our problem. More fundamental than the nucleon-nucleus cross section is the nucleon-nucleon one, since the first can be obtained in terms of the second. In order to understand that, let us consider a primary proton colliding with a nucleus of A nucleons. Due to the short range of hadron interaction, the proton will interact with only some of nucleons of the target. The number of such "wounded" nucleons can be estimated by simple geometrical considerations considering the path of the projectile inside the nucleus. The main relevant parameters are the nucleon–nucleon cross section, the size of the nucleus and its nuclear density. At high energy, since the binding energy of a nucleon is only of the order of 8 MeV, the incoming proton interacts independently with each of these wounded nucleons. All this is mathematically described by the Glauber multiple scattering formalism(Glauber and Matthieu, 1970). In that treatment, we end up with an expression for nucleon-nucleus (and nucleus-nucleus) cross section which is just a function of total σ_{pp} total and of the amplitude of elastic scattering.

Very often, for instance to calculate uncorrelated fluxes, one makes use of inclusive cross sections for the process $p + A \rightarrow meson + X$: $E\frac{d^3\sigma}{dp^3}$ The cosmic ray interactions (and shower development) are often described in the laboratory frame, where the target (air) nucleus is at rest and the primary projectile has 4-momentum/nucleon $p \equiv (E_0/A, \vec{p})$. Therefore, remembering that the basic interaction is the nucleon-nucleon one, the corresponding center of mass energy (the one available for particle production) will be:

$$\sqrt{s} = \sqrt{m_n^2 + m_n^2 + 2m_n(E_0/A)} \sim \sqrt{2m_n(E_0/A)} \qquad (1)$$

We can verify that the knee region corresponds to about $\sqrt{s} = 1\ TeV$, while the $10^{17}\ eV$ range corresponds to the c.m. energy of the future LHC p-p collider at CERN ($14\ TeV$). Up to a proton energy $E_p \sim 1000$ TeV pp interactions are covered by existing pp ($p\bar{p}$) collider experimental data. In the highest energy part of the region of interest, no direct collider measurements are available yet, and lower energy data have to be extrapolated. Nucleus-nucleus data from accelerator experiments need a much stronger extrapolation.

Looking at the gross feature of particle production in hadron interactions, the experiments show that the bulk of it consists of hadron emitted at limited transverse momentum with respect to the direction of the incident nucleon, ("soft" processes, with a typical $\langle P_t \rangle \sim 0.3\ GeV/c$, at low energy), which corresponds to the reciprocal of the transverse

size of hadrons; in these processes the momentum transfer between the beam and target particles is small. More rarely, high-P_t production occurs ("hard" scattering), and this can be understood and calculated in the framework of perturbative QCD on the basis of the lowest order Feynman graphs involving the elementary constituents of hadrons (quarks and gluons). In any case, most of the energy is carried away longitudinally. It was initially suggested by Feynman that the inclusive cross sections could be expressed by a product of functions, factorizing the longitudinal part with a universal (energy independent) transverse momentum distribution. Furthermore, also motivated by experimental results at low energy and in the framework of the description of hadrons as constituted by point-like elementary partons, he also suggested a scaling law for the longitudinal function, which should be a function of just one dimensionless variable, $x_{Feynman}$ or, simply x_F(Feynman, 1969):

$$E\frac{d^3\sigma}{dp^3} = F(\sqrt{s}, P^{cm}_{long}) \cdot G(P_t) = F\left(x_F = 2P^{cm}_{long}/\sqrt{s}\right) \cdot G(P_t) \tag{2}$$

The exact definition of x_F would be $P^{cm}_{long}/(P^{cm}_{long})^{Max}$, and is defined from -1 to 1.

We can re-express the invariant cross sections as:

$$E\frac{d^3\sigma}{dp^3} \sim x_F \frac{d^3\sigma}{dx_F dp_T^2} \tag{3}$$

Under the strongest hypothesis of Feynman scaling (*i.e.* that $f(x_F = 0, P_t) =$ constant), the height of the plateau of the rapidity distribution is also constant and does not depend on energy. Within this approximation, the inelastic total cross sections, and hence the scattering lengths are constant and the average number of particles grows logarithmically with the energy. In this case, the shower production can be described as a process in which a particle interacts every interaction length, producing an approximately constant number of secondaries per interaction. As a consequence, it is easy to show that the depth of shower maximum will increase logarithmically with primary energy. If instead scaling is strongly violated, with the multiplicity of secondary particles growing much faster than $\log s$, then, for a given total energy, the shower will develop earlier in the atmosphere, and the number of particles observed at sea level will be smaller.

The Feynman scaling is never completely valid, and with increasing energy such hypothesis is more and more violated: the cross section grows, and so does the height of the rapidity plateau. Scaling violations now find their explanation in the contribution of hard QCD scattering as a function of energy(Alpgard et al., 1981). However, the scaling hypothesis remains an useful attempt to understand the general behaviour of cosmic ray interactions. In fact, the relevant question for us is if such violations affect all the kinematic range useful for the description of cosmic ray production. The kinematic region for which x_F exceeds ~ 0.1 ("beam fragmentation" region), where secondary particles retain most of the momentum of the primary, turns out to be the most important kinematic region for secondary cosmic ray production in the atmosphere. Unfortunately, the high x_F distributions are experimentally measured only at lab energies of a few hundreds of GeV. In high energy hadron colliders, only the central region is generally inside the detector acceptance. Therefore, as far as high energy cosmic ray physics is concerned, we have to rely on the extrapolations to high x_F, under the guide of phenomenological models. However, it is a relevant experimental fact that the measurement of inclusive

secondary cosmic ray fluxes at very high energy, like TeV muons, do indicate that the amount of Feynman scaling violation is small. From experiment we also learn that the simple hypothesis of factorization between longitudinal and transverse momentum is not true in reality.

Speaking about extrapolations, we have to go back to the question of the consequences of considering nuclei instead of free nucleons. Both experiments and phenomenological models point out that pN interactions induce important modifications to the secondary production, as compared to the pp interactions at the corresponding c.m. energy. For instance, both multiplicity and transverse momentum distributions are affected by nuclear effects(Schmidt and Schukraft, 1992). Also in this case there is a lack of useful experimental data, especially in the fragmentation region, and once again one has to rely on models.

3 Building models for cosmic ray physics

In summary, the hadronic sector of high energy particle and nuclear physics, a part from the general acknowledgement of the centrality of color dynamics, is far from being successfully manageable as the electro-weak world. On the other hand, cosmic ray demands a model for hadronic and nuclear interactions capable of providing the basic hadronic interaction term for the cascade, i.e. the cross section for hadron-hadron, hadron-nucleus and nucleus-nucleus collisions as a function of energy. The model should work from the pion production threshold up to the highest possible primary energies. Perturbative QCD can be used in practice only for high $P_\perp$ phenomena. Even if the role of hard scattering becomes noticeable at the knee energy, and essential at the highest observed energies, the calculation of the bulk of the interactions necessarily addresses the non-perturbative range. Unfortunately, there are not yet exact ways to calculate the bulk of soft, non-perturbative, interactions, and one has to rely on phenomenological models. In any case, results from collider and fixed target experiments at accelerators provide important informations for a hadron production model to be used at cosmic ray energies.

A rather remarkable success seems to be achieved by theoretically inspired models such as the Dual Parton Model(Capella et al., 1987) or the Quark Gluon String model(Kaidalov et al., 1982) (the latter is traditionally diffused in the east-european countries). Both make similar use of concepts derived from the mathematical requirements of scattering theory, as unitarity and analyticity (Regge theory) and also color flow and parton idea and topological expansion of QCD. In practice, however, many different variations exist of these basic models; also, many different practical implementation exist in different numerical codes. Other differences may come from the different way of merging DPM with perturbative QCD.

3.1 The DPMJET–II model

In the framework of the two component Dual Parton Model (DPM), the hadron production in hadron-hadron collisions is dominated, at first order, by soft interactions (pomeron exchange) between valence quarks and di–quark of projectile and target, with a contribution, increasing with energy, of hard interactions (gluon–gluon scattering). The extension to hadron–nucleus and nucleus–nucleus collisions is obtained by means of multiple, soft

and hard, interactions, involving at first order also sea quarks from both projectile and target. An implementation of this scenario is performed in the the DPMJET-II Monte Carlo (Ranft, 1995). A description of this has been presented also at a previous edition of this conference(Ranft, 1994). The model predicts a rather good Feynman scaling in the fragmentation region as far as inelastic, non–diffractive interactions are concerned, as shown in Fig. 1. Violation of scaling occurs in the central region, mostly driven by QCD contributions. However, it must be stressed that scaling violations occurs also near $x_F = 1$ for leading baryon production, due to diffractive scattering, as shown in Fig. 2. This behaviour is typical of all models of this class. As partly suggested by the model itself, the amount of diffractive scattering reaches a constant plateau with energy, while the rest of inelastic cross section increases.

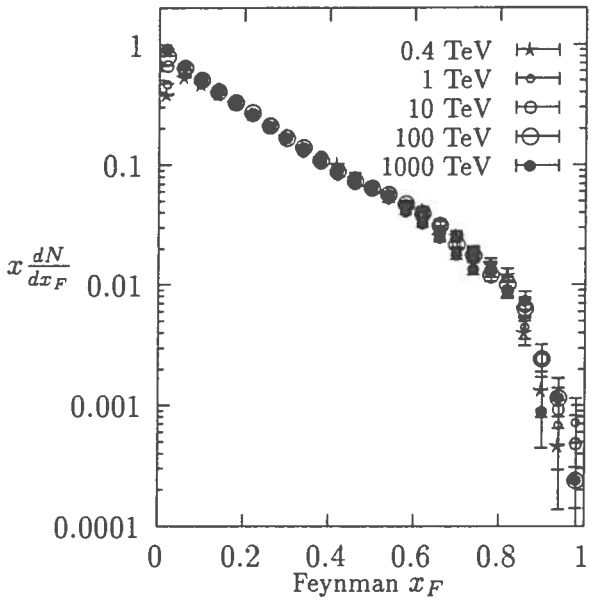

Figure 1: Test of Feynman scaling for π^+ production in proton–proton collisions as calculated with DPMJET–II.

This event generator has been used for sampling cosmic ray cascades interfaced to the HEMAS code (Battistoni et al., 1995).

In the following, we shall focus the discussion on the nucleus–nucleus interactions and their implementation in DPMJET–II. A great effort has been devoted to the development of this model in the case of nuclear projectile and target. This is of fundamental importance for the high energy cosmic ray physics, since the extrapolation from hadron-hadron to nucleus-nucleus physics for $\sqrt{s} > 1$ TeV will be hard to achieve on the basis of accelerator physics.

3.2 The nucleus–nucleus interaction at high energies

The MC model for nucleus-nucleus (and hadron-nucleus) interactions starts from the spatial initial configuration, i.e. the positions of the nucleons in space-time in the rest system of the corresponding nucleus, which is sampled from standard density distributions. For energies above 3-5 GeV/nucleon the collision proceeds via ν elementary interactions

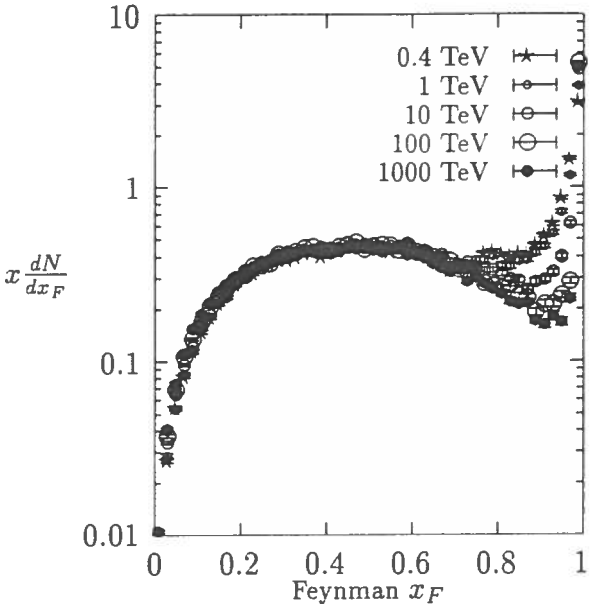

Figure 2: Test of Feynman scaling for leading baryons in proton–proton collisions as calculated with DPMJET–II.

between ν_p and ν_t nucleons from the projectile and target, respectively. The values ν, ν_p, and ν_t are sampled according to Glauber's multiple scattering formalism using the MC algorithm of (Shmakov et al., 1989). The particle production is well described by the two-component DPM which is applied as in hadron-hadron interactions (Aurenche et al., 1992). As a result, a system of color strings ("chains") connecting partons (valence and/or sea quarks) of the nucleons involved in the scattering process is formed. The chains are hadronized applying the JETSET model (Sjöstrand, 1992). The hadrons may then cause intranuclear cascade processes.

The DPM for nucleus–nucleus collisions differs from the superposition model. There are three main reasons for these differences:
1) In A–B collisions according to DPM with full Glauber cascade we have ν^{A-B}, ν_t^{A-B} and ν_p^{A-B} all different from one. In Fe-Air collisions we have usually $\nu^{A-B} > \nu_p^{A-B} > \nu_t^{A-B}$. In this situation, the simplest possibility is to form ν_t^{A-B} valence–valence chain pairs, $\nu_p^{A-B} - \nu_t^{A-B}$ valence–sea chain pairs and $\nu^{A-B} - \nu_p^{A-B}$ sea–sea chain pairs. In the superposition model for the A–B collision, we have ν_p^{A-B} nucleon–B collisions where $\nu^{n-B} = \nu_t^{n-B}$ and $\nu_p^{n-B} = 1$. Therefore in the superposition model for the A–B collision we obtain ν_p^{A-B} pairs of valence–valence chains and $\nu_p^{A-B}(\nu_t^{n-B} - 1)$ pairs of sea–valence chains. There are never any sea–sea chains in the superposition model. These are instead replaced by sea-valence chains, thus artificially involving too many valence-quarks of the target.
2) all spectators in the full DPMJET–II appear among the final state particles, either as evaporation protons or neutrons or as nuclear fragments and residual nuclei. We are not able to define nuclear fragments and residual nuclei in the superposition model.
3) The possible inclusion of a Formation Zone Intranuclear Cascade (FZIC). This process has been included only recently(Battistoni et al., 1996), together with a much more refined model for nuclear fragmentation(Ferrari et al., 1996), and it will be described in some

detail in the following.

Before introducing the discussion on FZIC, it is useful to give an example of the measurable differences between different choices in the interaction models. In Table 1 we show the the number of atmospheric muons with E_μ >1 TeV as produced by DPMJET–II for primary protons and Fe nuclei at different energies, using the full nucleus-nucleus interaction. These numbers are compared with what is obtained switching to the superposition model (of course non difference exists for protons), and to the results of the purely phenomenological HEMAS code(Forti et al., 1990), based on the parameterization of collider results, using the cross sections from the "semi–superposition" model of NUCLIB (Engel et al., 1992), mainly adopted in the SIBYLL interaction model(Fletcher et al., 1994). We notice how the muon yield increases, in the lowest region of energy/nucleon, when moving from the superposition model to the full nucleus–nucleus interaction. The "semi–superposition model" is an interesting approach, since one the main effects of nucleus–nucleus interaction, namely the different interaction height of nuclei with respect to free nucleons, is taken into account, but the dynamics of the interaction remains that of nucleon–nucleus.

Table 1: Yields of atmospheric muon above 1 TeV for DPMJET for full nucleus– nucleus interaction, superposition model and the HEMAS code.

A	E/nucleon (TeV)	No. of Show.	HEMAS	DPMJET superp.	DPMJET
1	3	560000	1285	2256	-
56	3	10000	1297	2738	3425
1	10	280000	15363	16301	-
56	10	5000	15232	15931	19962
1	100	56000	36645	35849	-
56	100	1000	35648	35646	35810
1	1000	11200	40306	40622	-
56	1000	200	40325	41009	40090

In Fig.3 we show the calculated e.m. size spectrum, in the region below the knee, at the atmospheric depth of 810 g/cm^2 (~2000 m a.s.l.) as produced by vertical protons with the energy spectrum $E^{-2.86}$, for DPMJET, HEMAS and SIBYLL. All interaction models are embedded in the same shower code (HEMAS), where the shower size has been computed using the parameterizations of GEANT results (Patera et al., 1995).

Due to the limits of this review, a complete discussion of other aspects, like $P_\perp$ production and transverse structure of the showers is not possible. It is anyway important to mention how the DPMJET model has been optimized as far as all relevant nuclear effects are concerned. In particular, it includes the known Cronin effect (Cronin et al., 1975) on the $P_\perp$ enhancement in hadron–nucleus and nucleus–nucleus collisions. Careful check with experimental data has been performed. This concept will be briefly rediscussed later.

It is also interesting to compare some basic ingredients of different models. For instance, in Table 2 we compare at two different energies the *pp* and nucleus–nucleus cross sections for He-Air and Fe-Air interactions, together with the average number of elementary collisions, as resulting from Glauber calculations, in DPMJET and NUCLIB. Noticeable differences can be found.

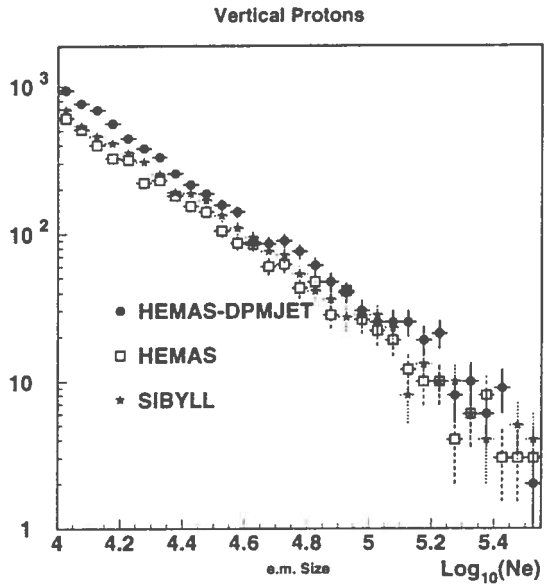

Figure 3: Calculated e.m. size spectrum, in the region below the knee, at the atmospheric depth of 810 g/cm^2 (~2000 m a.s.l.) as produced by vertical protons with the energy spectrum $E^{-2.86}$, for DPMJET, HEMAS and SIBYLL.

3.3 The formation zone cascade in target and projectile nuclei

In the FZIC model, one defines an average formation time τ_s to create a hadronic state in the rest system of a secondary hadron of mass m_s and transverse momentum $p_{s\perp}$ is introduced(Ranft, 1989):

$$\tau_s = \tau_0 \frac{m_s^2}{m_s^2 + p_{s\perp}^2}. \tag{4}$$

where $\tau_0 = 4.5$ fm/c is a parameter determined by comparing the computed results to the experimental data. For each secondary, a formation time τ is sampled from an exponential distribution with average value τ_s.

Due to relativistic time dilatation, those secondaries having sufficiently high energy in the rest frame of the considered nucleus are formed mostly outside of the spectator part of this nucleus, whereas those with lower energies are formed inside. The latter may initiate an intranuclear cascade in the spectator. The $P_\perp$ enhancement (Cronin effect) mentioned before is associated to the concept of formation zone: those partons who travel in the nucleus before starting hadronization, undergo a sort of QCD multiple scattering which affects the final $P_\perp$ value(Hüfner et al., 1988).

In p–air collisions, in the target fragmentation region, at x_F values between -0.3 and -1, significant differences in the distributions due to the pions produced by the formation zone cascade in the target nucleus are found. It may be important to point out that Feynman–x_F in h–A and A–A collisions is defined with the longitudinal momentum in the hadron-nucleon (or nucleon-nucleon) center of mass system p_z^{cms} as $x_F = p_z^{cms}/|p_{z,max}^{cms}|$ where $p_{z,max}^{cms}$ is calculated disregarding Fermi momenta.

Now, turning to nucleus–air collisions, the intranuclear cascade is developed both in target and projectile. Due to the Lorentz boost from the c.m. system to the laboratory

Table 2: Examples of Nucleus–nucleus cross sections and average number of elementary collisions, as resulting from Glauber calculations, in DPMJET and NUCLIB. Input values for σ_{pp} are also shown.

1) He-Air Collision						
$\sqrt{s}$=1000 GeV						
DPMJET–II						
σ_{pp}^{inel}	σ_{pp}^{el}	$< \nu >$	$< \nu_p >$	$< \nu_t >$	σ_{AB}^{inel} $(\sim \sigma_{AB}^{prod})$	
55.0	12.40	4.45	2.32	3.42	753.0	
NUCLIB						
σ_{pp}^{inel}	σ_{pp}^{el}	$< \nu >$	$< \nu_p >$	$< \nu_t >$	σ_{AB}^{prod}	$\sigma_{AB}^{quasi-el.}$
54.5	19.98	5.12	2.33	3.25	595.0	78.0
$\sqrt{s}$=100000 GeV						
DPMJET–II						
σ_{pp}^{inel}	σ_{pp}^{el}	$< \nu >$	$< \nu_p >$	$< \nu_t >$	σ_{AB}^{inel} $(\sim \sigma_{AB}^{prod})$	
96.6	35.8	6.51	2.58	4.33	935.0	
NUCLIB						
σ_{pp}^{inel}	σ_{pp}^{el}	$< \nu >$	$< \nu_p >$	$< \nu_t >$	σ_{AB}^{prod}	$\sigma_{AB}^{quasi-el.}$
110.9	90.9	7.52	2.57	4.01	826.0	241.0
Fe-Air Collision						
$\sqrt{s}$=1000 GeV						
DPMJET–II						
σ_{pp}^{inel}	σ_{pp}^{el}	$< \nu >$	$< \nu_p >$	$< \nu_t >$	σ_{AB}^{inel} $(\sim \sigma_{AB}^{prod})$	
55.0	12.40	21.36	11.86	6.90	2135.0	
NUCLIB						
σ_{pp}^{inel}	σ_{pp}^{el}	$< \nu >$	$< \nu_p >$	$< \nu_t >$	σ_{AB}^{prod}	$\sigma_{AB}^{quasi-el.}$
54.5	19.98	28.72	13.02	6.94	1674.0	114.0
$\sqrt{s}$=100000 GeV						
DPMJET–II						
σ_{pp}^{inel}	σ_{pp}^{el}	$< \nu >$	$< \nu_p >$	$< \nu_t >$	σ_{AB}^{inel} $(\sim \sigma_{AB}^{prod})$	
96.6	35.8	36.16	15.42	7.79	2422.0	

system, now the intranuclear cascade in the projectile gives interesting features for secondary cosmic ray production. In the case of light nuclei, like He, the formation zone cascade really makes no difference and can be neglected. For heavy nuclei the situation is different. Such differences are also visible in the projectile fragmentation region at positive x_F values, but here those differences, not significant in the case of He–air collisions, rise instead with the mass number of the projectile nucleus. For instance, in Fig. 4, the Feynman–x_F distribution of π^+ in Fe–air collisions at a lab–energy of 500 TeV per projectile nucleon is shown for DPMJET with and without FZIC.

As a consequence, while for He–air collisions the model agrees practically to the model without formation zone cascade, for Fe–air, in the x_F region relevant for secondary cosmic ray production, differences are up to 50% from the superposition model. These differences might be significant at the level of the first interaction in the cosmic ray cascade, but only after full shower calculations one can draw conclusions on a possible significative difference

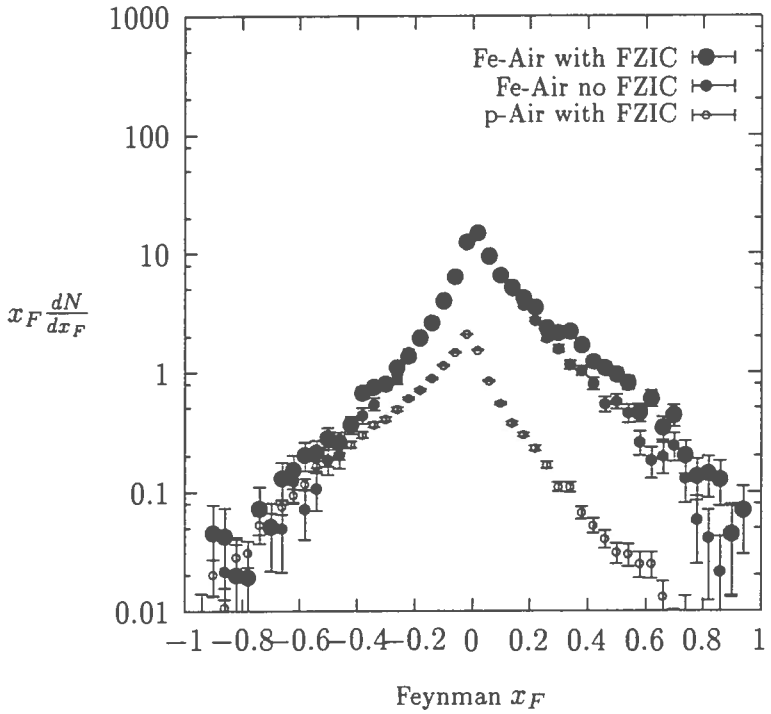

Figure 4: Feynman-x_F distribution of π^+ in Fe–air collisions at a lab–energy of 500 TeV per projectile nucleon. Plot 1 (large full circles) is for the full model with FZIC in the target and projectile nucleus; plot 2 (small full circles) is for the model without FZIC. For comparison, also the same distribution in p–air collisions with FZIC (small empty circles) is given.

on typical observables.

The model with FZIC predicts a more enhanced yield of nucleons and light fragments than the model without FZIC(Ferrari et al., 1996). This fact probably attenuates the possible differences in full shower calculations with respect to superposition model. Some preliminary evaluation has been performed comparing Fe-Air interactions at from 10^{14} to 10^{16} eV/nucleus, with and without FZIC. Differences are small. In particular, in the model with FZIC, one gets:
1) the e.m. size is smaller by $\Delta Log_{10} N_e = 0.02 \div 0.05$;
2) the yield of secondary high energy muons ($E_\mu > 1$ TeV) is smaller by $9 \div 11\%$, but their energy spectrum is practically unchanged.

4 Discussion about a few uncertainties

There are many aspects in the field of hadronic interactions that are source of uncertainty, in general and within a particular model. At the end of this review, we wish to focus the attention on a few of them:
a) beyond the already quoted uncertainty in the inelastic cross sections, it must be stressed how data on single diffractive cross sections are not sufficient to put reliable constraints on the models about the quantitative weight of such a kind of collision. As shown before, diffraction determines most of the breaking of Feynman scaling at high x_F, and therefore also the inelasticity of a model, i.e. the fraction of energy taken away in the collision by the non-leading particles. Inelasticity affects the longitudinal development of the hadronic shower.

b) There are different opinions on the role of hard scattering (minijets) and of their evolution as a function of c.m. energy. It must be pointed out how the question is strictly linked, from the point of view of the energetics of the model, to the structure functions of partons inside nucleons(Ranft, 1994 and 1995), i.e. the functions giving the probability to find inside a nucleon a parton with a given fraction of nucleon momentum. In the DPMJET model, after the first experimental results at HERA, the set of structure functions MRSD- has been chosen(Martin et al., 1993). Due to the strong divergence ($\sim 1/x^{1.5}$) at low x of these structure functions, the correct unitarization of hard and soft cross contributions puts a limit to the maximum energy affordable by the model around 10^{18} eV. However, more recent data, suggest less steep structure functions(Glük et al., 1993). The uncertainty in these structure functions is not very relevant in the knee regions, but can lead to non negligible differences both in the total inelastic cross section and charged multiplicity for $\sqrt{s}$ exceeding 10 TeV, in correspondence of the Extreme High Energies of cosmic rays.
c) One should ask which consequences can be envisaged for cosmic ray physics in the knee region, if the changes in nuclear collisions as seen in the recent heavy-ion experiments at CERN are confirmed. (threshold in J/ψ suppression in central Pb-Pb collisions, changes in dileptons and strangeness production). Such changes, if true, should lead to effects also for collisions of ions lighter than Pb, at sufficiently high energy.

5 Acknowledgments

The author is indebted to C. Forti, J. Ranft for the fruitful collaboration. A. Ferrari, P. Lipari and T.K. Gaisser are thanked for the several enlightening discussions on the argument.

6 References

Alpgard, K. et al.: 1981, *Phys. Lett.* **B107** 310.
Aurenche, P. et al.: 1992, Phys. Rev. **D45** 92.
Battistoni, G. et al.: 1995, Astroparticle Phys. **3** 157.
Battistoni, G. et al.: 1996, Preprint Univ. Santiago de Compostela, US-FT / 29-96.
Capella, A. et al.: 1994, Phys. Rep. **236** 227 and references therein.
Cronin, J. et al., 1975: Phys. Rev. **D11** 3105.
Engel, J. et al.: 1992, Phys. Rev. **D46** 5013.
Ferrari, A. et al.: 1996, Zeit.Phys. **C70** 413 and Zeit. Phys. **C71** 75.
Feynman, R.P.: 1968, Phys. Rev. **23** 1415.
Forti, C. et al.: 1990, Phys. Rev. D **42** 3668.
Fletcher , R.S. et al.: 1994 Phys. Rev **D50** 5710.
Glauber, R.J and Matthiae, G: 1970 *Nucl. Phys.* **B21** 135.
Glück, M. and Reya, E. and Vogt, A.: 1992, Phys. Rev. **D45** 3986.
Kaidalov, A.B. et al.: 1982, Phys. Lett. **B116** 459.
Hüfner J. et al.: 1988, Phys. Lett. **B215** no. 2, 218.
Martin, A.D. and Roberts, R.G. and Stirling, W.J.: 1993, Phys. Rev. **47** 867.
Patera V. et al.: 1995, Nucl. Instr. and Meth. **A356** 514.
Ranft, J.: 1989, Zeit. Phys. **C43** 439.
Ranft, J.: 1994, Proceedings of the Vulcano Workshop 1994.
Ranft, J.: 1995, Phys. Rev. **D51** 64.
Shmakov, S.Yu., et al.: 1989, Comp. Phys. Comm. **54** 125.
Schmidt, H.R. and Schukraft, J.: 1992, GSI–preprint GS I–92–19.
Sjöstrand, T.: 1992, CERN Report CERN–TH.6488/92.